Electronic Supplementary Material (ESI) for Nanoscale.

Hybridization between plasmonic and photonic modes in laser-induced self-organized quasi-random plasmonic metasurfaces

*Van Doan Le[1], Yaya Lefkir[1], Nathalie Destouches[1]**

[1]Univ Lyon, UJM-Saint-Etienne, CNRS, Institut d'Optique Graduate School,

Laboratoire Hubert Curien UMR 5516, F-42023 Saint-Etienne, France.

**Corresponding author: nathalie.destouches@univ-st-etienne.fr*

1. Size distribution.

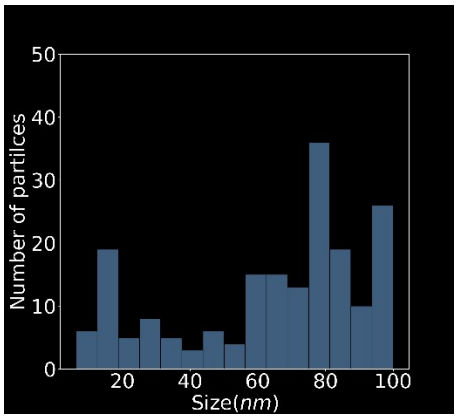

Figure S1. Size distribution of the sample irradiated by the laser at wavelength of 488 nm, power of 250 mW and scan speed of 300 μm/s.

2. Chemical components and Raman spectrum of the sample.

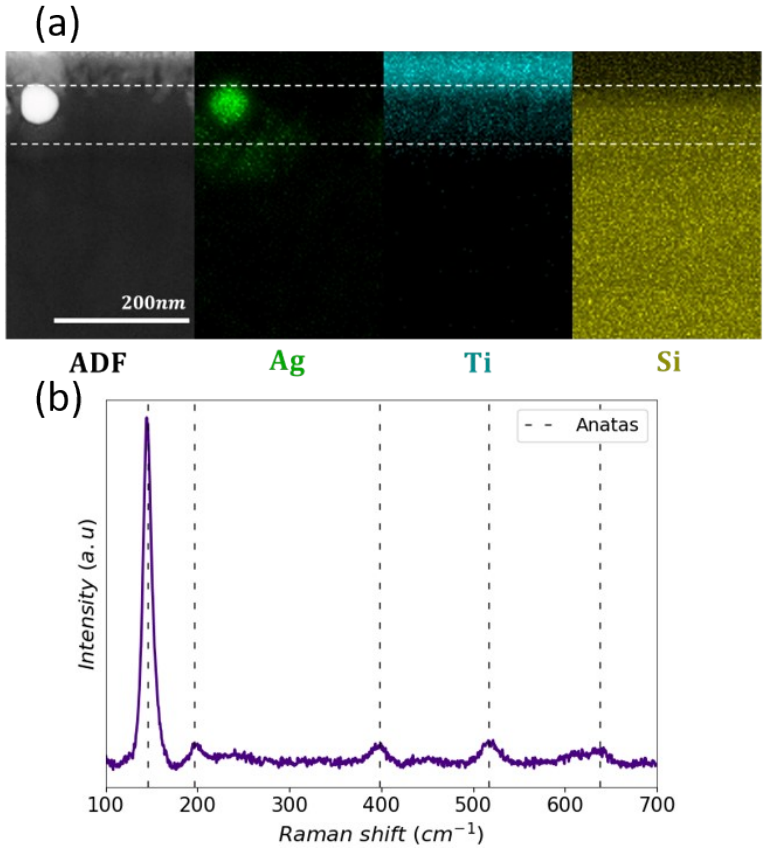

Figure S2. Characterization of the sample illuminated by laser at 488 nm, power = 250 mW and scan speed = 300 μm/s (a) Chemical analysis of the sample cross-section by annular dark field (ADF) electron microscopy and energy-dispersive spectroscopy that highlights Ag, Ti and Si atomic content. Dashed white lines indicate the layer interface. (b) Raman spectrum of the sample after background removal.[1,2]

3. Optimization of the intermediate layer (n_2)

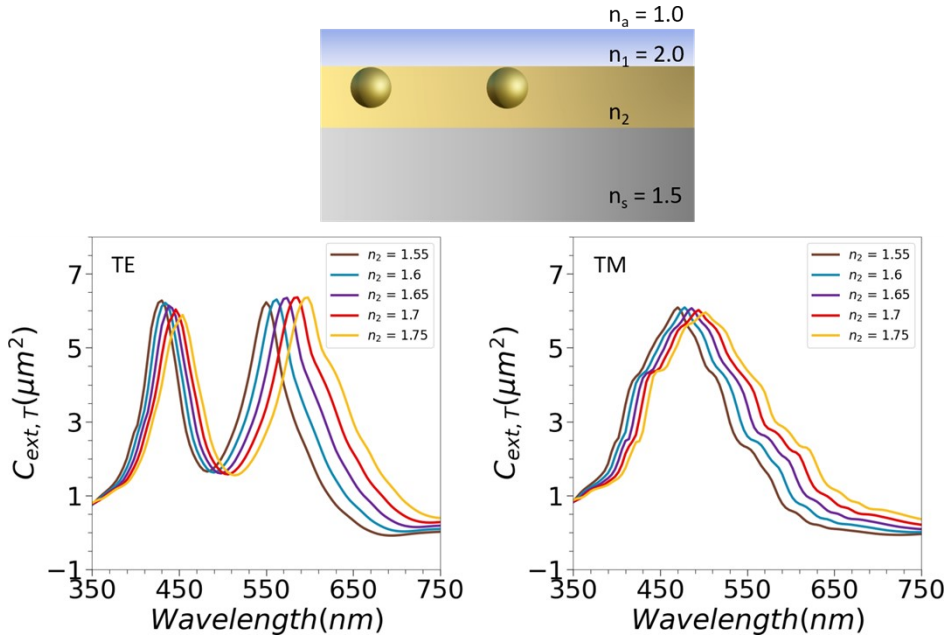

Figure S3. Extinction cross-section in transmission side of TE and TM polarization of the as-fabricated sample when varying refractive index of the intermediate layer. The refractive index $n_2 = 1.65$ is chosen since it provides the closest match to the measured results.

4. Extinction of experiment and simulation.

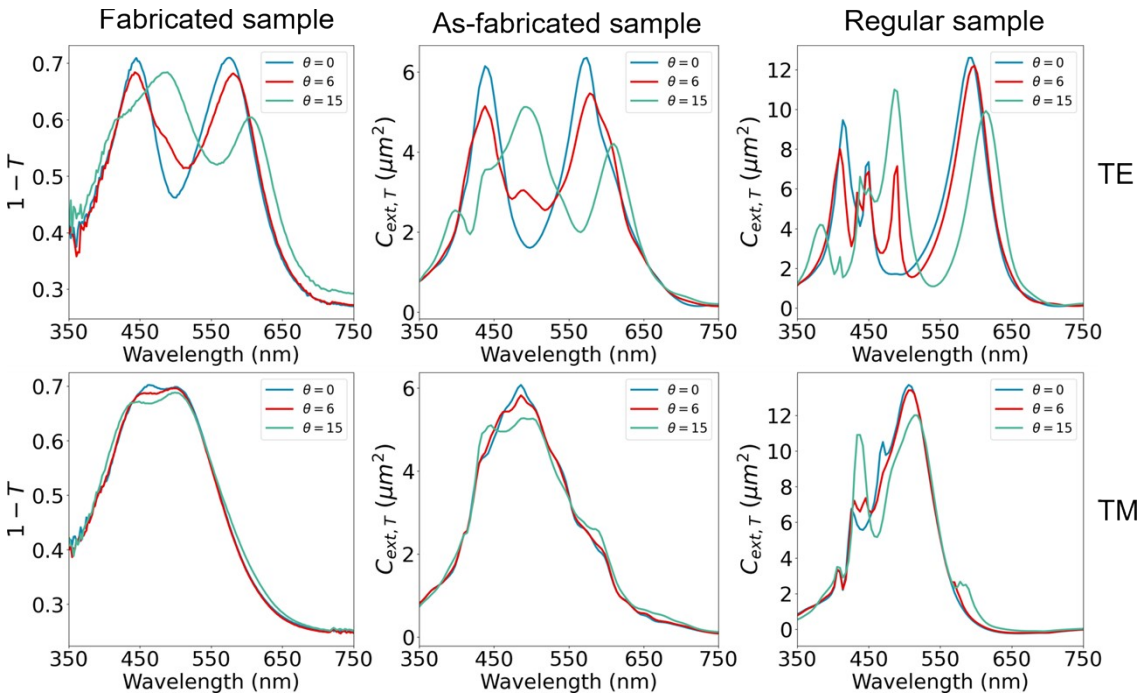

Figure S4. Experimental extinction of the fabricated sample (1 - T) and simulated extinction cross-section in transmission side of the as-fabricated and regular samples for TE and TM polarization under different incidence angles. The sample is described in Supplementary Figure S1.

5. Multipole extraction of as-fabricated sample and regular sample.

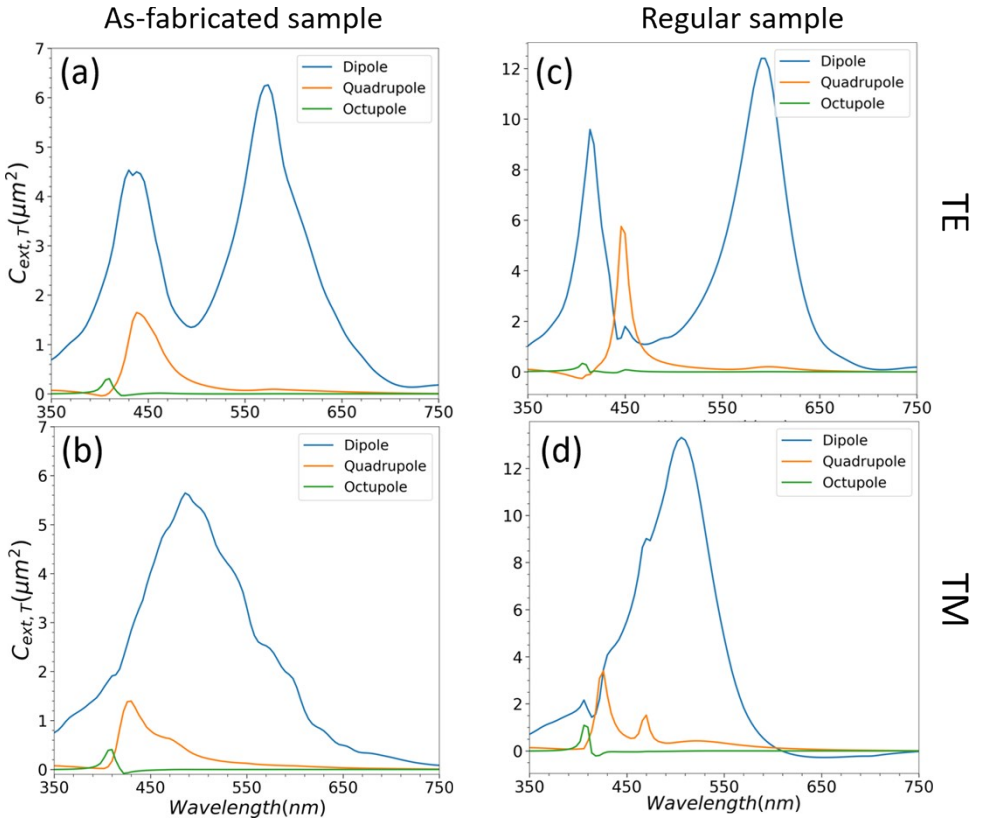

Figure S5. Multipole decomposition of the extinction cross-section for TE and TM polarization of as-fabricated sample (a-b) and regular sample (c-d) respectively.

6. Positional disorder and nanoparticle array.

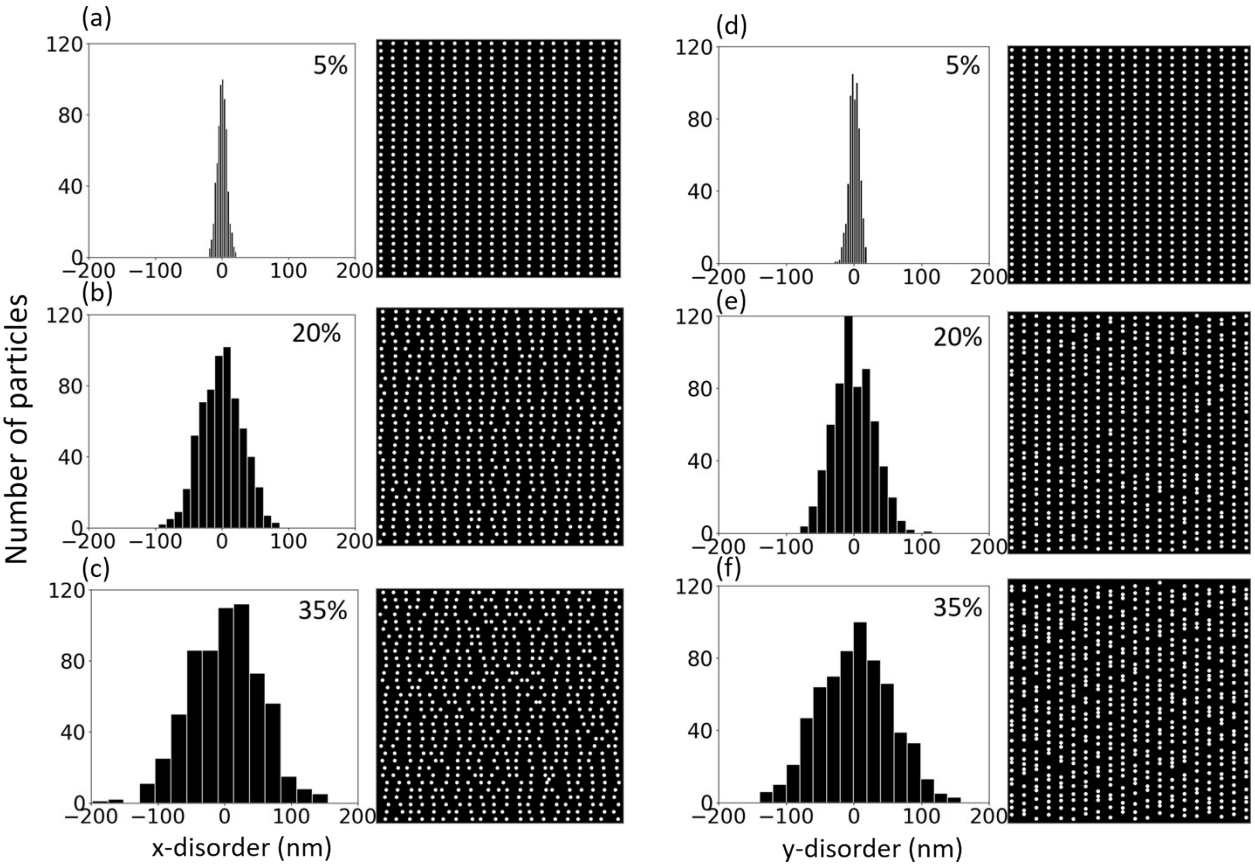

Figure S6. Introduction of disorder in the regular structure. Histogram of the distance from the periodic array of the nanoparticle center along x or y and the spatial distribution of silver nanoparticles in the simulated structure. The disorder is increasing from the top to the bottom row by broadening the position histograms (5 – 35%) for x-disorder (a, b, c) and y-disorder (d, e, f), respectively.

7. Effect of size distribution

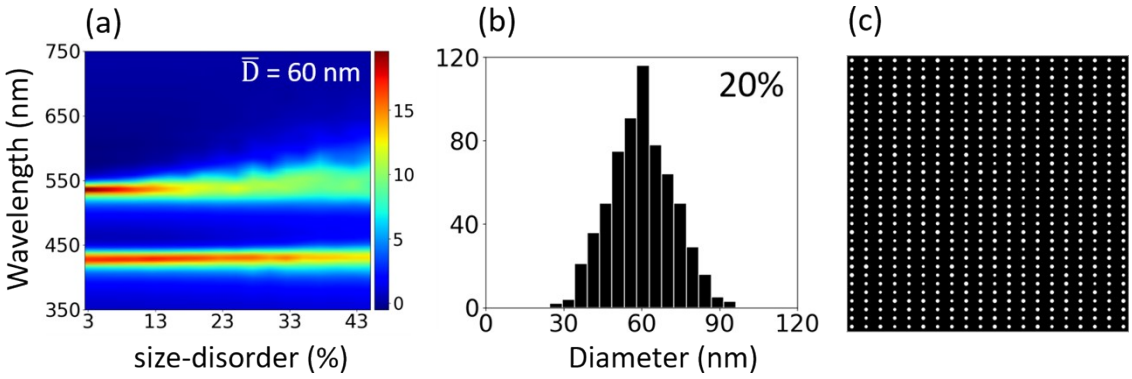

Figure S7. (a) Extinction efficiency for size distribution with the mean diameter of 60 nm. (b, c) Histogram and nanoparticle array of 20% size disorder, respectively. The higher disorder corresponds to broader histogram. When varying the size, we keep the regular position of nanoparticles.

8. Spectral variation for array of NP = 10 x 16

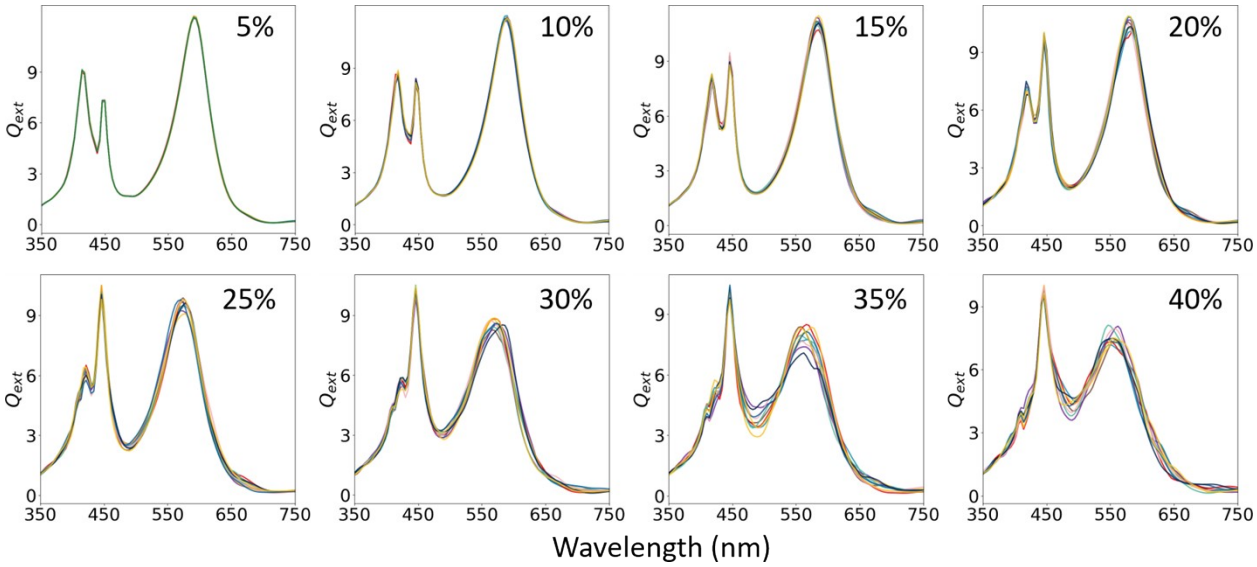

Figure S8. Spectral variation of ten simulations for array of NP = 10 x 16 with increasing x-disorder (5% - 40%).

9. Spectral variation for array with increasing size at x-disorder = 20%

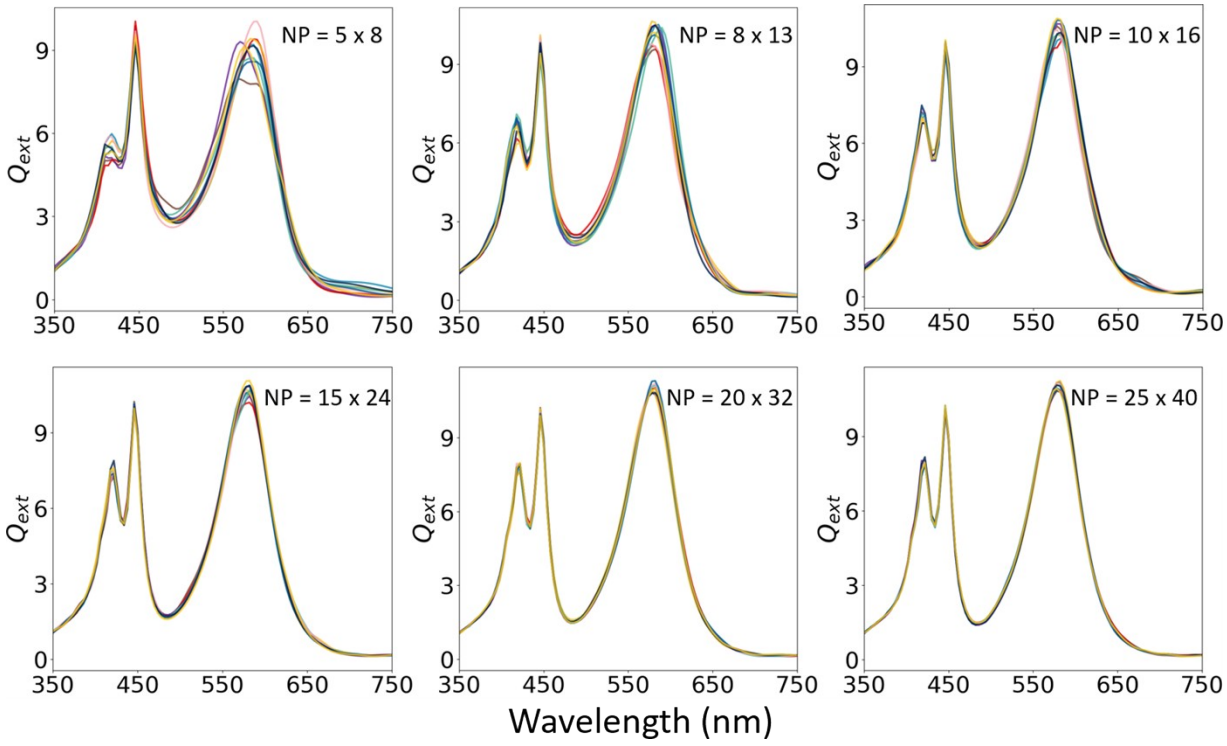

Figure S9. Spectral variation of ten simulations for array with increasing size from NP = 40 to NP = 1000 at x-disorder = 20%.

10. Quantify the spatial disorder of as-fabricated sample

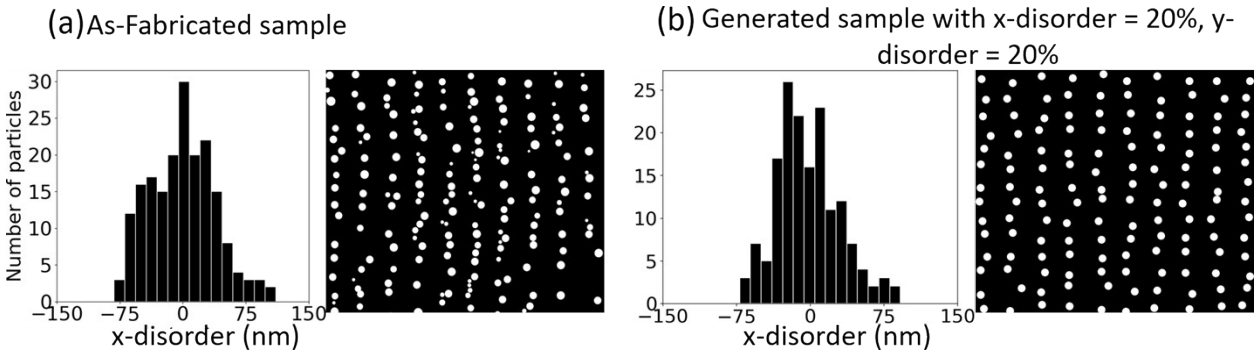

Figure S10. Histogram and nanoparticle array. (a) for as-fabricated sample and (b) for a generated sample with x-disorder = 20% and y-disorder = 20%.

11. Simulation of the as-fabricated nanoparticle array in a homogeneous medium

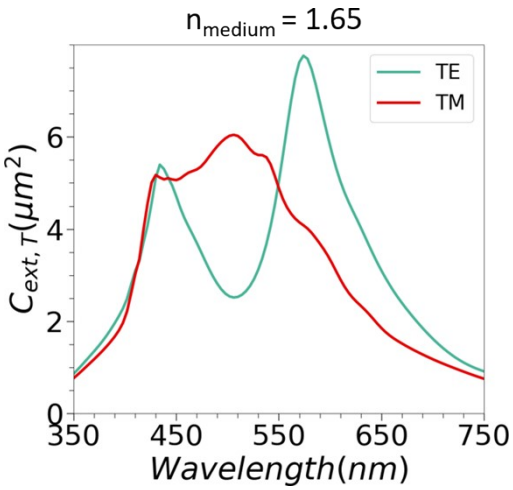

Figure S11. Extinction cross-section in transmission side of the as-fabricated nanoparticle array (as shown in Figure 1d) embedded in a homogeneous medium with n = 1.65. TE, TM indicate incident polarizations oriented parallel and perpendicular to the grating lines respectively.

12. Extinction cross-section and nearfield distributions for TM polarization.

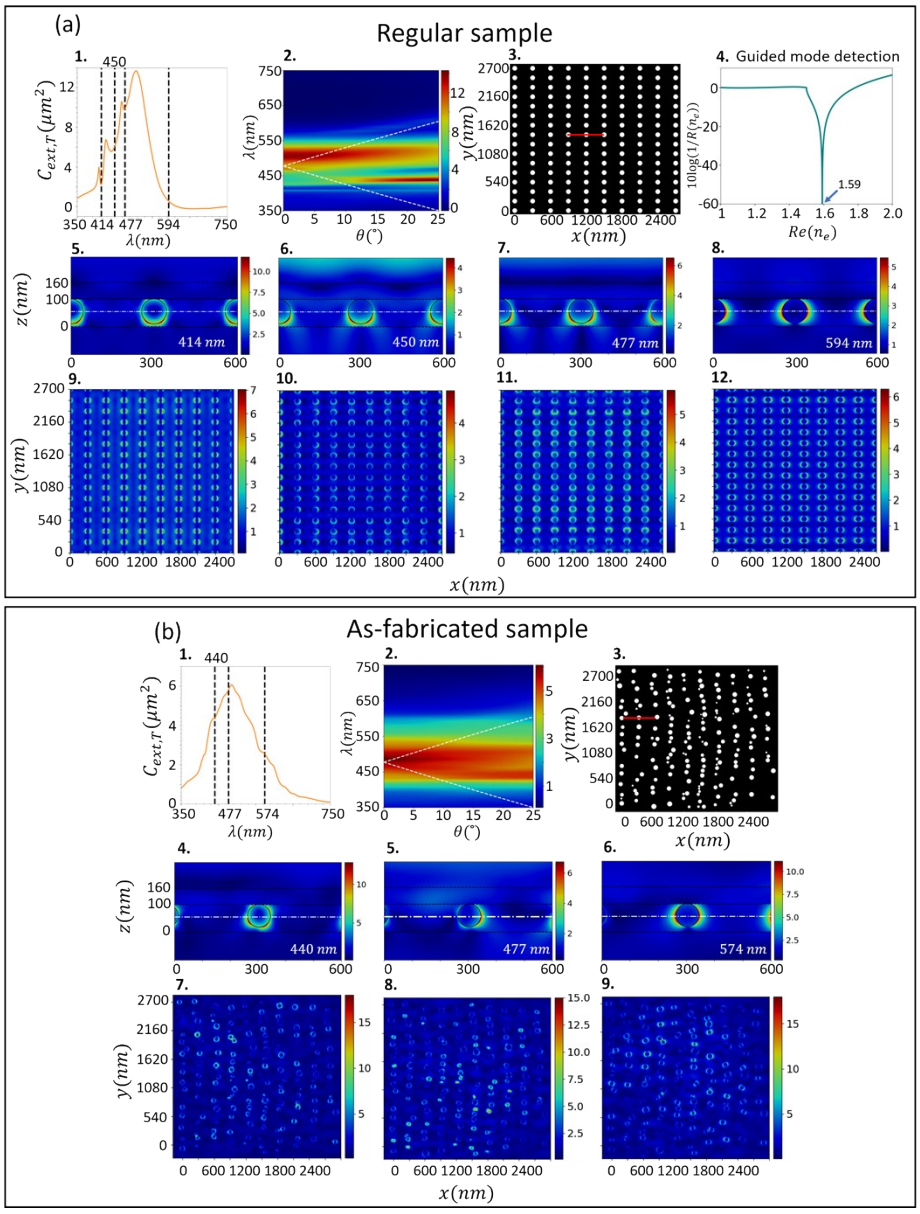

Figure S12. Spectral variations of $C_{ext,T}$ under normal incidence for (a.1) the regular and (b.1) as-fabricated sample. The vertical dotted lines indicate the wavelengths at which the near field is calculated below. Spectral and angular maps of $C_{ext,T}$ for (a.2) the regular and (b.2) as-fabricated sample. The white dashed lines indicate the guided modes excited by ± 1 diffraction orders. Plan-view of the (a.3) regular and (b.3) real-like NP arrays. (a.4) Pole of the reflection coefficient R of the two-layer system without nanoparticles. (a.5-12, b.4-9) cross-section and

plan-view of the near field intensity distribution at selected wavelengths (shown in fig. a.1 and b.1 respectively). The nearfield intensities shown in plan-view are calculated on the white dashed dotted lines drawn in the cross-section pictures. The nearfield intensities shown in cross-section are calculated on the red lines in figure a.3 and b.3. The black dashed lines indicate the layer interfaces. All calculations are implemented for TM polarization.

13. Extinction in transmission side with incident plane is parallel to the yz-plane.

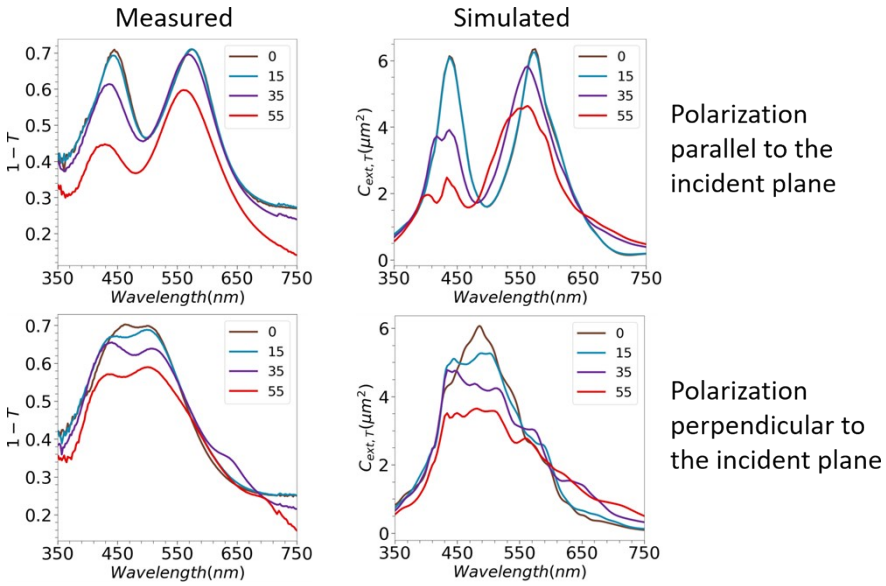

Figure S13. Extinction in transmission side of measured and simulated samples for two incident polarizations at different incident angle. The incident plane is parallel to the yz-plane.

14. Nearfield intensity at the middle of TiO_2 layer under normal incidence.

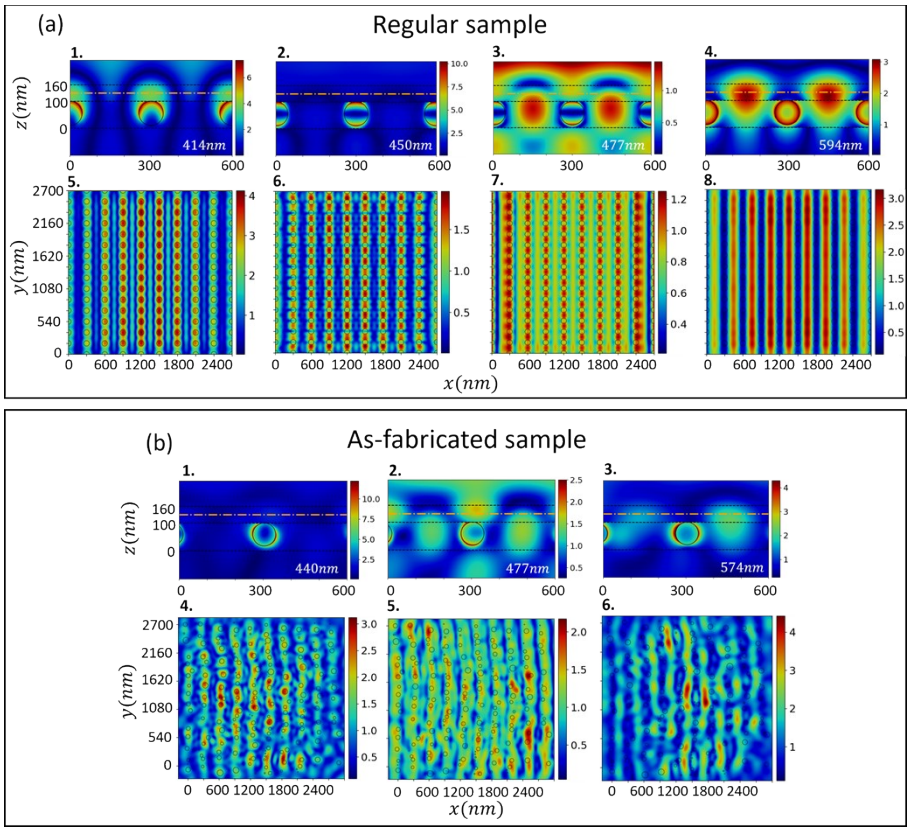

Figure S14. (a-b) Nearfield intensity on cross-section and plan-views (z = 130 nm) at the selected wavelengths, where the spectra exhibit extinction dips or peaks as shown in Figure 3, under normal incidence of the regular sample and real-like sample respectively. The orange dashed dotted lines in cross-section view indicate where the plan-views are calculated. The black circles in plan-views represent the NPs positions and sizes.

15. Effect of layer thickness on the coupling.

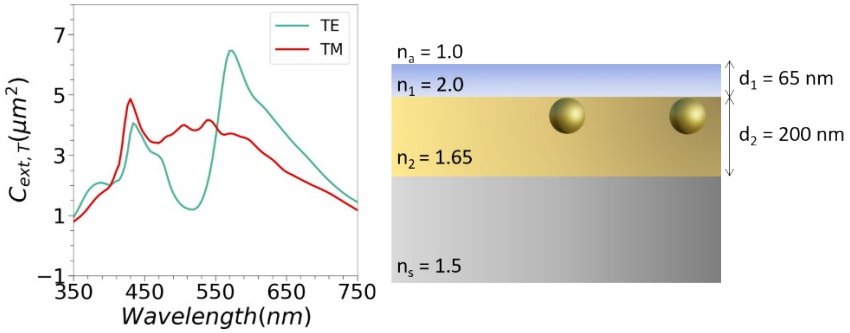

Figure S15. Extinction cross-section in transmission side of the as-fabricated sample (Figure 1d in the manuscript) simulated with thicker layer of $n_2 = 1.65$ for TE and TM polarization.

1.6 SEM picture in cross-section and size distribution of the sample illuminated by laser at 647 nm, power = 500 mW and san speed = 300 μm/s.

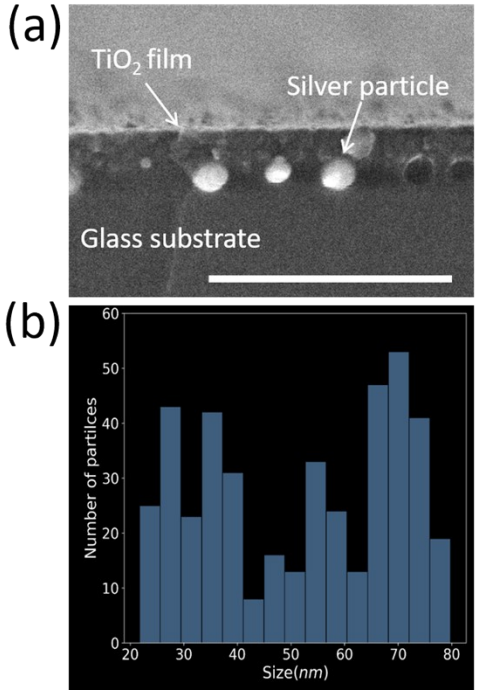

Figure S16. (a) Cross-section view and (b) size distribution of the sample processed by laser at 647 nm, 500 mW and 300 μm/s. The scale bar is 500 nm

11. References

(1) Eilers, P. H. C. A Perfect Smoother. *Anal. Chem.* **2003**, *75*, 3631–3636.

(2) He, S.; Zhang, W.; Liu, L.; Huang, Y.; He, J.; Xie, W.; Wu, P.; Du, C. Baseline Correction for Raman Spectra Using an Improved Asymmetric Least Squares Method. *Anal. Methods* **2014**, *6*, 4402–4407.